

Creep and shrinkage behavior of high-strength concrete and minimum reinforcement ratio for bridge columns

**Halit Cenan Mertol,
Sami Rizkalla, Paul Zia,
and Amir Mirmiran**

The use of high-strength concrete (HSC) in bridges and buildings has become increasingly common. HSC increases the load-carrying capacity of the columns and allows for a reduction of column cross-sectional area in buildings. In bridges, the use of prestressed HSC girders results in cost savings, either from a reduction in the number of girders or from an increase in the span length. This study is aimed specifically at the use of HSC for bridge structures.

Under applied stresses, time-dependent creep deformation develops in hardened concrete. There are two types of creep of concrete:

- basic creep, which occurs under constant moisture conditions
- drying creep, which is the additional creep that occurs due to a moisture loss from the ambient conditions

Drying creep involves the combined effect of shrinkage and creep, whereas basic creep is an independent process.

Editor's quick points

- Current creep and shrinkage prediction equations used for bridge design were derived from research on high-strength concrete (HSC) with compressive strengths up to 12 ksi (83 MPa).
- This paper summarizes the findings of an extensive research program on the creep and shrinkage behavior of HSC with strengths up to 18 ksi (124 MPa).
- The authors also examine the applicability of bridge-design creep and shrinkage prediction equations for HSC up to 18 ksi.

Table 1. Test matrix for creep

Set	Rack	Target concrete strength, ksi	Curing type	Concrete strength at 28 days, ksi	Concrete age at loading, days	Concrete strength at loading, ksi	Applied stress, ksi
1	10Rack1	10	1-day heat	10.4	1	9.6	2 (0.2 f'_c)
	10Rack2		7-day moist	12.1	14	10.8	
	10Rack3				28	12.1	
	10Rack4				8	8.3	4 (0.4 f'_c)
	10Rack5		14	10.8			
	10Rack6		28	12.1			
2	14Rack1	14	1-day heat	14.3	1	12.8	2.8 (0.2 f'_c)
	14Rack2		7-day moist	15.7	14	14.5	
	14Rack3				28	15.7	
	14Rack4				7	11.4	5.6 (0.4 f'_c)
	14Rack5		14	14.5			
	14Rack6		28	15.7			
3	18Rack1	18	1-day heat	14.4	1	11.4	3.6 (0.2 f'_c)
	18Rack2		7-day moist	16.7	14	15.0	
	18Rack3				28	16.7	
	18Rack4				7	12.0	7.2 (0.4 f'_c)
	18Rack5		14	15.0			
	18Rack6		28	16.7			

Note: f'_c = compressive strength of concrete. 1 ksi = 6.895 MPa.

The volume of hardened concrete reduces in time due to the loss of moisture content known as shrinkage. There are three types of concrete shrinkage:

- Drying shrinkage occurs because of the loss of moisture content from hardened concrete under drying conditions. This process is partially irreversible. Even if the concrete is placed in a high-humidity environment, not all of the drying shrinkage will be prevented.
- Autogenous (chemical) shrinkage occurs because of the removal of internal water as a result of the hydration of the cement.
- Carbonation shrinkage occurs because of the carbonation of the hydration products in the presence of carbon dioxide in a low–relative humidity *RH* environment.

Information on creep and shrinkage of concrete is necessary to determine the prestress losses, long-term deforma-

tions, and cracking of prestressed concrete structures. Many current code equations for creep and shrinkage predictions are based on normal-strength concrete. Due to the lack of research data on the creep and shrinkage characteristics of HSC, many design codes limit its use for concrete structures.

The creep and shrinkage prediction methods specified by the American Association of State Highway and Transportation Officials' *AASHTO LRFD Bridge Design Specifications*¹ were based on the research conducted by Tadros et al.² The equations used in the methods of Tadros et al. were compared with those in the available domestic and foreign literature, including methods currently used for creep and shrinkage predictions. The estimated results from Tadros et al. produced more-accurate and realistic estimates than those provided by the existing methods in the literature.

This paper summarizes the findings of an extensive research program to examine the shrinkage and creep behav-

Table 2. Test matrix for shrinkage

Set	Specimen	Curing type	Specimen type	Target concrete strength, ksi	
1	10SP1	1-day heat	Prismatic	10	
	10SP2				
	10SP3				
	10SP4				
	10SP5	7-day moist			
	10SP6				
	10SC1				Cylindrical
	10SC2				
2	14SP1	1-day heat	Prismatic	14	
	14SP2				
	14SP3				
	14SP4				
	14SP5	7-day moist			
	14SP6				
	14SC1				Cylindrical
	14SC2				
3	18SP1	1-day heat	Prismatic	18	
	18SP2				
	18SP3				
	18SP4				
	18SP5	7-day moist			
	18SP6				
	18SC1				Cylindrical
	18SC2				

Note: 1 ksi = 6.895 MPa.

ior of HSC with strengths up to 18 ksi (124 MPa), extending the database of Tadros et al. The creep and shrinkage predictions derived from the current AASHTO LRFD specifications and the predictions' applicability to HSC for concrete strengths up to 18 ksi (124 MPa) were examined.

Experimental investigation

The test program consisted of 42 cylindrical specimens measuring 4 in. × 12 in. (100 mm × 300 mm) and 18 prismatic specimens measuring 3 in. × 3 in. × 11¼ in. (75 mm × 75 mm × 290 mm). Thirty-six cylindrical specimens were used to determine the creep of HSC, of which two specimens were used in each creep test. Six cylindrical specimens and the eighteen prismatic specimens were used to evaluate the shrinkage of HSC. **Tables 1** and **2** show the test matrix for this program.

Materials

Logan³ developed mixture proportions (**Table 3**) for the three target concrete compressive strengths of 10 ksi, 14 ksi, and 18 ksi (69 MPa, 97 MPa, and 124 MPa).

The coarse aggregate used in all mixtures was crushed stone with a nominal maximum size of ¾ in. (10 mm). Depending on the target compressive strength, one of two types of fine aggregate was used: natural sand or manufactured sand. The cement was Type I/II and the mixture included silica fume, fly ash, a high-range water-reducing admixture (HRWRA), and a retarding admixture to reduce the water-cement ratio *w/c* and enhance workability.

Three 4 in. × 8 in. (100 mm × 200 mm) cylinders were tested for each specimen to determine the compressive strength at the time of testing.

Test method and setup

Two different curing conditions were used in this investigation: 1-day heat curing and 7-day moist curing. The 1-day heat curing simulated the fabrication process in precast, prestressed concrete plants. Half an hour after casting, specimens for 1-day heat curing were placed in an environmental chamber for 24 hr, where the temperature was controlled to achieve internal concrete temperatures from 150 °F to 160 °F (66 °C to 71 °C). The cylindrical molds were covered with plastic lids and the prismatic molds were wrapped with wet burlap and plastic sheets to prevent moisture loss throughout the heat-curing process. At the end of 24 hr, the specimens were removed from the molds and stored in the laboratory, where the temperature was maintained at about 72 °F (22 °C) with 50% RH.

The 7-day moist curing represented typical curing procedures for reinforced concrete members. These specimens were kept in molds at room temperature for 24 hr. The cylindrical molds were covered with plastic lids, and the prismatic molds were covered with wet burlap and plastic sheets to prevent moisture loss. After 24 hr, the specimens were removed from their molds and submerged in a water-curing tank. The water temperature in the curing tank was maintained at 73.5 °F ± 3.5 °F (23 °C ± 2 °C)

using specially designed heaters equipped with adjustable thermostats. The water was saturated with lime to prevent leaching of calcium hydroxide from the test specimens. The curing tanks also contained pumps that circulated the water to maintain a constant temperature and concentration of calcium hydroxide throughout the tank. At the age of 7 days, the specimens were removed from the curing tanks and stored in the laboratory, where the temperature was maintained at about 72 °F (22 °C) with 50% RH.

Figure 1 shows the setup of the creep tests performed using the 4 in. × 12 in. (100 mm × 300 mm) cylindrical specimens. Two identical cylindrical specimens were stacked and concentrically loaded in each creep rack equipped with a 60-kip-capacity (270 kN) hydraulic jack. The cylinders were ground at both ends to ensure uniformity of the applied axial load. Two different stress levels of 0.2 f'_c and 0.4 f'_c were used, where f'_c is the target compressive strength of concrete. The applied load in each creep rack was monitored by a pressure gauge connected to the hydraulic jack at the time of loading and strain gauges attached to the three threaded rods of each rack.

Six demountable mechanical (DEMEC) inserts embedded in each concrete cylinder on three 120-deg-angle planes along the longitudinal axis measured the concrete strain with an 8 in. (200 mm) DEMEC gauge. One-day heat-cured specimens were loaded at the end of the curing period, whereas three different groups of the 7-day moist-cured specimens were loaded at ages 7 days, 14 days, or 28 days.

A data logger continuously monitored the load in each creep rack. Disk springs maintained the load in the creep racks to minimize the load reduction due to creep and shrinkage of concrete. If the load reduction exceeded 5% of the specified load in any rack, the load was adjusted using the hydraulic jack to the initial specified value. The creep specimens had companion shrinkage specimens from which the shrinkage strain of the 4 in. × 12 in. (100 mm × 300 mm) cylinders was determined. These shrinkage-strain readings were deduced from the DEMEC readings to obtain the net creep strain of the specimens. The two ends of the cylindrical shrinkage specimens were sealed with epoxy to simulate the same volume-to-surface ratio V/S of the loaded creep cylinders.

Prismatic specimens, 3 in. × 3 in. × 11¼ in. (75 mm × 75 mm × 290 mm), were also used to measure the shrinkage strain in accordance with ASTM C157.⁴ Figure 1 shows the test setup. Two inserts were embedded at the top and the bottom of each specimen to monitor the shrinkage strain using a dial indicator. The tests for 1-day heat-cured specimens were started at the end of the first day, whereas the tests for the 7-day moist-cured specimens were started at an age of 7 days.

The measurements from the creep and shrinkage specimens were recorded at the predetermined time intervals for two years, with more-frequent readings occurring within the first three months of the testing period.

Table 3. Mixture designs for three target concrete compressive strengths

Material	Target concrete compressive strengths		
	10 ksi	14 ksi	18 ksi
Cement, lb/yd ³	703	703	935
Silica fume, lb/yd ³	75	75	75
Fly ash, lb/yd ³	192	192	50
Sand, lb/yd ³	1055 [†]	1315 [‡]	1240 [‡]
Rock, lb/yd ³	1830	1830	1830
Water, lb/yd ³	292	250	267
High-range water-reducing admixture, fl oz/cwt*	17	24	36
Retarding admixture, fl oz/cwt*	3	3	3
Water–cementitious materials ratio	0.30	0.26	0.25
28-day compressive strength, ksi	11.5	14.4	17.1

* fl oz per 100 lb of cementitious materials

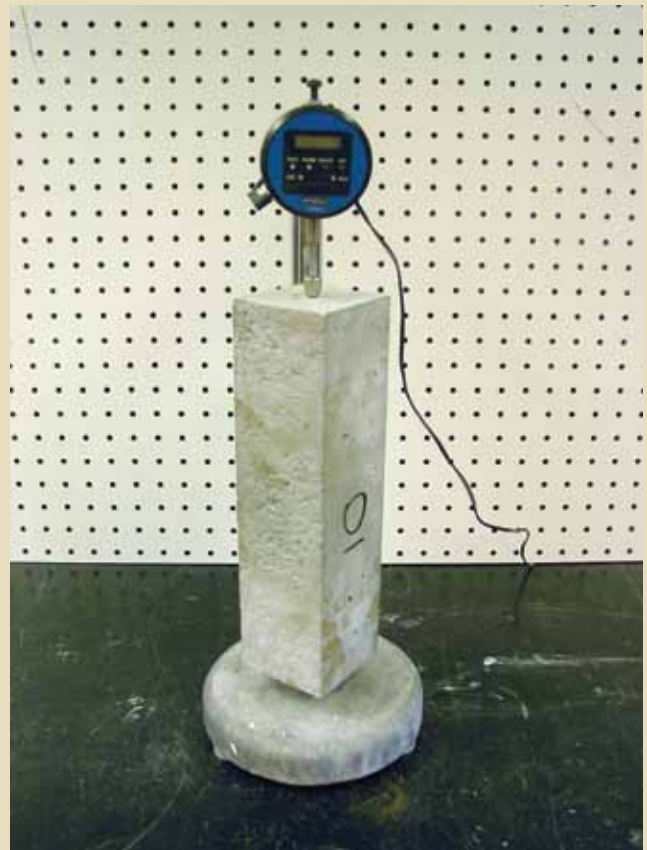
[†] Natural sand

[‡] Manufactured sand

Note: 1 yd = 0.914 m; 1 fl oz = 29.6 mL; 1 lb = 0.453 kg; 1 ksi = 6.895 MPa.



Creep test



Shrinkage test

Figure 1. Creep tests were performed using the 4 in. × 12 in. cylindrical specimens, and shrinkage tests used 3 in. × 3 in. × 11¼ in. prismatic specimens. Note: 1 in. = 25.4 mm.

Experimental results and discussions

Test results were compared with the predicted creep and shrinkage according to the AASHTO LRFD specifications. **Table 4** lists the creep and shrinkage prediction equations given by the AASHTO LRFD specifications.

It may be of interest that the equation for modulus of elasticity E_c includes a factor K_1 to account for the effect of aggregate type. Given that creep and shrinkage are known to be affected by aggregate type, such effects could also be accounted for by introducing adjustment factors (such as K_2 and K_3) in the equations for creep coefficient ψ and shrinkage strain ϵ_{sh} , provided that sufficient research data are available to establish these factors. Such an approach may be particularly useful for precast, prestressed concrete producers and state departments of transportation when certain types of aggregates are known to be regularly used. Using such adjustment factors would provide better predictions of modulus of elasticity, creep coefficient, and shrinkage strain for design.

For this research program, the temperature of the surrounding environment was constant throughout the testing

period. However, the RH of the ambient air varied for this duration. Therefore, the creep and shrinkage-strain measurements were normalized by dividing them by the appropriate humidity factor (Table 4). An incremental procedure was used to adjust the measured data to 70% RH for comparison purposes. Mertol gives details of this procedure.⁵

Creep behavior

The creep strain was determined based on the measured total strain reduced by the measured shrinkage strain of the unloaded companion cylinders and the initial elastic strain of each creep cylinder. The creep coefficients, defined as the ratios of the creep strain at time t to instantaneous elastic strain, were calculated to evaluate the creep behavior for HSC.

The average creep coefficients presented for each concrete compressive strength and each stress level were based on average normalized values using two cylinders in each rack. The measured creep strains were adjusted to 70% RH , as explained previously. **Figure 2** compares the average creep coefficients of the creep specimens with the creep coefficient predictions using the AASHTO LRFD

Table 4. Current 2004 requirements for creep coefficient, shrinkage strain, and longitudinal reinforcement ratio by the AASHTO LRFD specifications

Description	Equation
Modulus of elasticity E_c	$E_c = 33,000K_1w_c^{1.5}\sqrt{f'_c}$
Creep coefficient ψ	$\psi(t, t_i) = 1.90k_{td}k_{ia}k_s k_{hc}k_f$
Shrinkage strain ϵ_{sh}	$\psi(t, t_i) = 1.90k_{td}k_{ia}k_s k_{hc}k_f$
Time-development factor k_{td}	$k_{td} = \frac{t}{61 - 4 \times f'_{ci} + t}$
Humidity factor k_{hs} and k_{hc}	$k_{hs} = 2.00 - 0.0143RH$ for shrinkage strain, $k_{hc} = 1.56 - 0.008RH$ for creep coefficient
Size factor k_s	$k_s = \frac{1064 - 94V/S}{735}$
Concrete strength factor k_f	$k_f = \frac{5}{1 + f'_{ci}}$
Loading-age factor k_{ia}	$k_{ia} = t_i^{-0.118}$ for creep coefficient only
Maximum longitudinal reinforcement ratio for compression members	$\frac{A_s}{A_g} + \frac{A_{ps}f_{pu}}{A_g f_y} \leq 0.08$ and $\frac{A_{ps}f_{pe}}{A_g f'_c} \leq 0.30$
Minimum longitudinal reinforcement ratio for compression members	$\frac{A_s f_y}{A_g f'_c} + \frac{A_{ps} f_{pu}}{A_g f'_c} \geq 0.135$

Note: A_g = gross area of the section; A_{ps} = area of prestressing steel; A_s = area of mild compression steel; f'_c = concrete compressive strength in ksi; f'_{ci} = specified compressive strength at prestress transfer for prestressed members or 80% of the strength at service for nonprestressed members in ksi; f_{pe} = effective prestress after losses; f_{pu} = specified tensile strength of prestressing steel; f_y = yield strength of mild steel; K_1 = correction factor for source of aggregate (taken as 1.0); RH = relative humidity of the ambient air in percentage; t = age of concrete after loading in days; t_i = age of concrete when load is initially applied for accelerated curing or the age minus 6 days for moist curing in days; V/S = volume-to-surface ratio in inches; w_c = density of concrete in kip/ft³.

specifications. Only the typical behavior for each concrete compressive strength is presented in these figures because of space limitations.

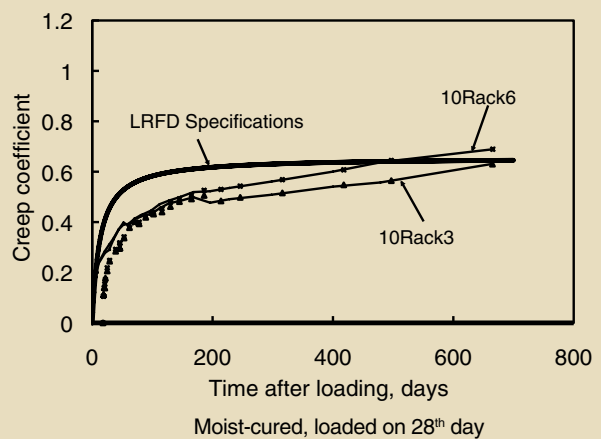
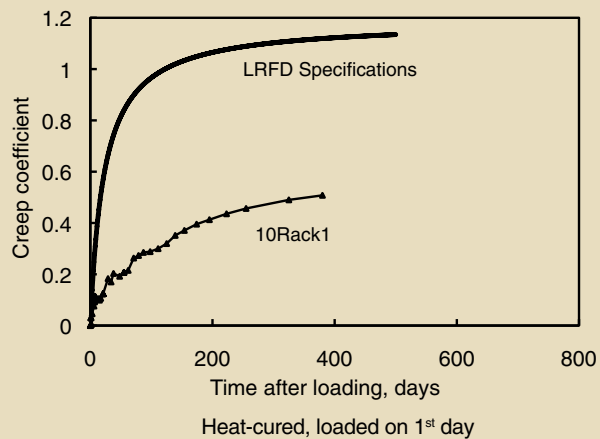
In general, the test results indicated that the creep behavior of HSC is similar to that of normal-strength concrete, where the creep rate decreases as time increases. For the same concrete compressive strength, the creep of the 1-day heat-cured cylinders was less than that of the 7-day moist-cured cylinders. As with normal-strength concrete, the creep for HSC is proportional to the applied stress, provided that the applied stress is less than the proportional limit.

The creep coefficient predicted by the AASHTO LRFD specifications was closer to the measured value for moist-cured HSC specimens but overestimated the measured value for heat-cured HSC specimens. However, it is noted that the predictions by the AASHTO LRFD specifications were consistently greater than the measured values, in some cases by a significant amount. A review of the research re-

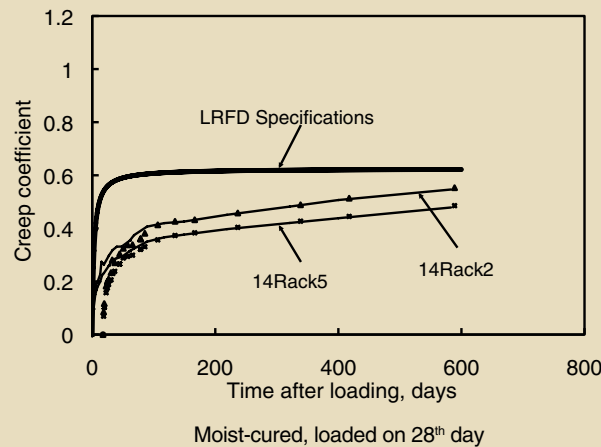
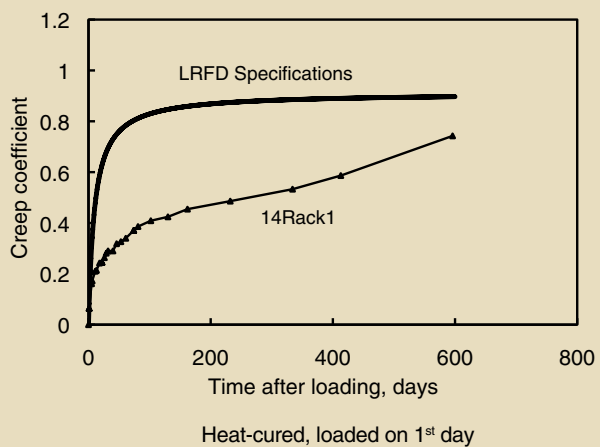
ported by Tadros et al.² indicates that the predictive equations proposed by them (Table 4) also overestimated their own five sets of data for HSC by a substantial amount, with standard deviations ranging from 29% to 51%.

In addition, the relationships specified by the AASHTO LRFD specifications were found to be reasonable to predict the creep behavior of HSC except for the time-development correction factor k_{td} (Table 4) that produced negative values in the first few days after loading if the concrete compressive strengths were greater than 15 ksi (103 MPa). For example, if f'_{ci} is 16 ksi (110 MPa), the value of k_{td} would be negative for t less than three days. For t equal to three days, the value of k_{td} would become infinity.

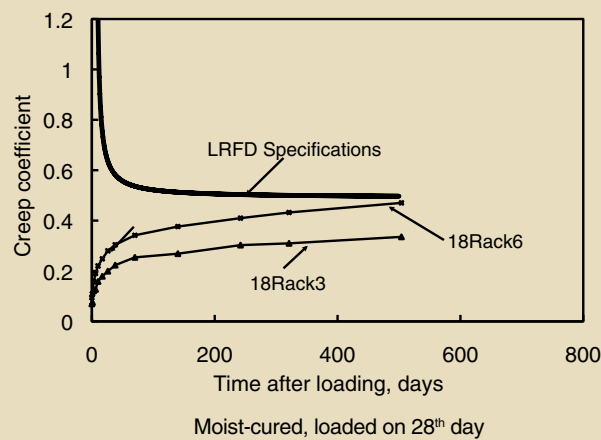
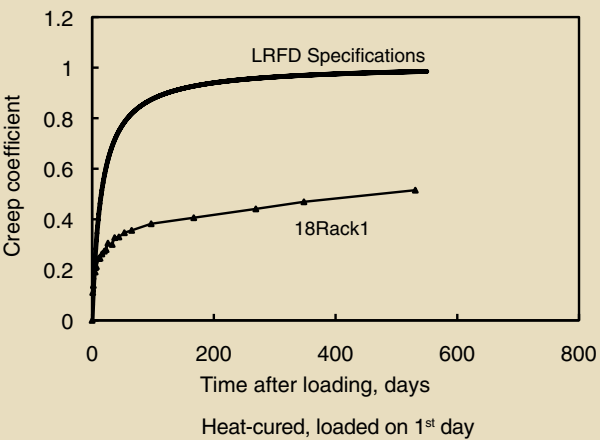
The equation also gives rapidly increasing values of k_{td} (more than one can reasonably expect) in the first few days for concrete compressive strengths greater than 12 ksi (83 MPa). Tadros et al. developed this equation based on research data with concrete compressive strengths up to 12



Set 1 specimens



Set 2 specimens



Set 3 specimens

Figure 2. These graphs compare the average creep coefficients of the specimens to the creep coefficient predictions using the American Association of State Highway and Transportation Officials' *AASHTO LRFD Bridge Design Specifications*.

ksi, and those data were extrapolated to include strengths up to 15 ksi (103 MPa). In terms of design, although concrete compressive strength of more than 15 ksi is unlikely

to be used as a transfer strength for pretensioned concrete members, it is possible that the strength could be achieved at the time of loading for cast-in-place concrete columns

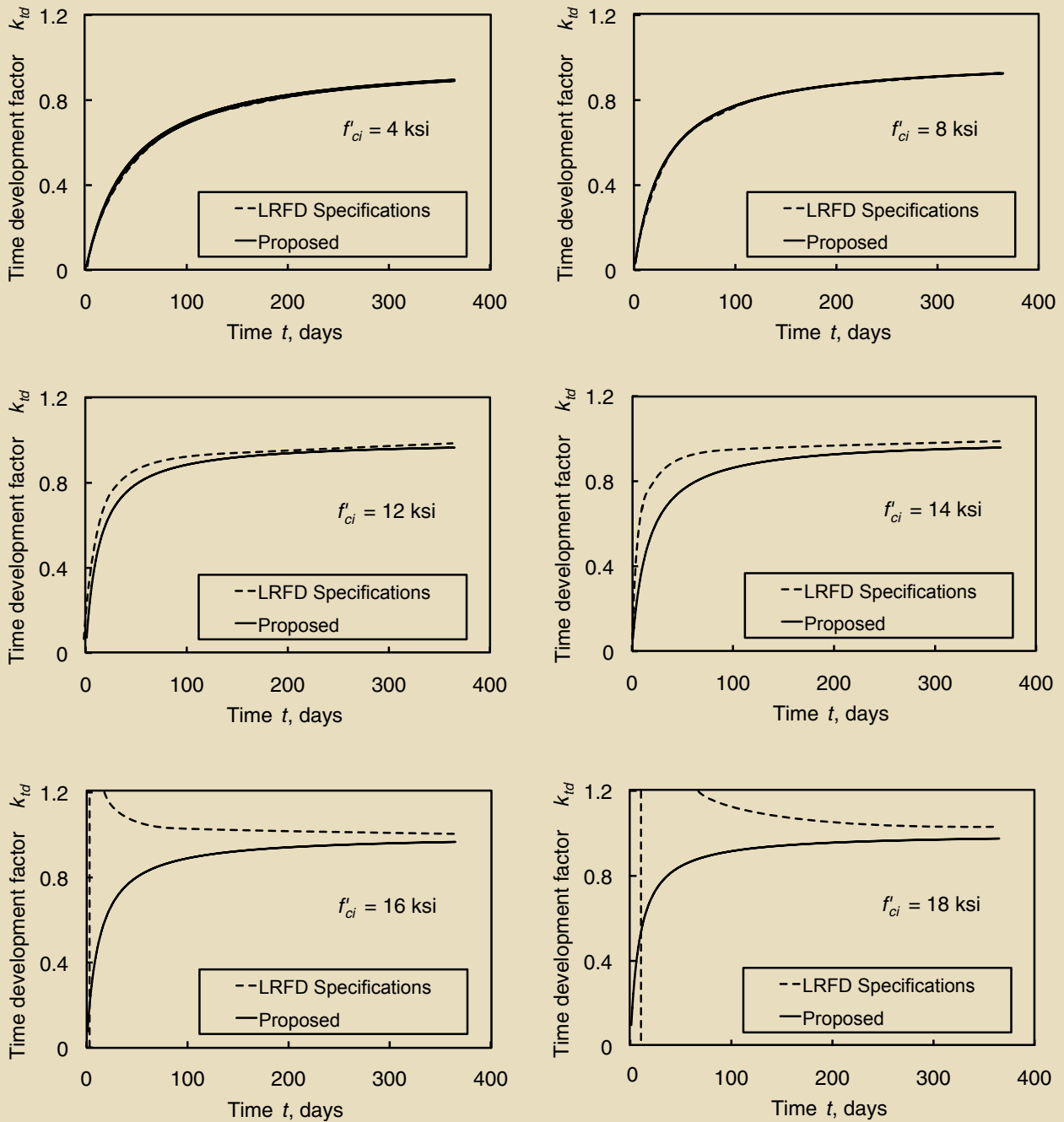


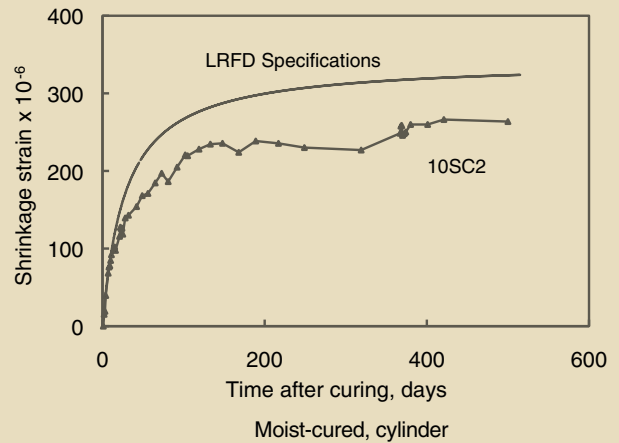
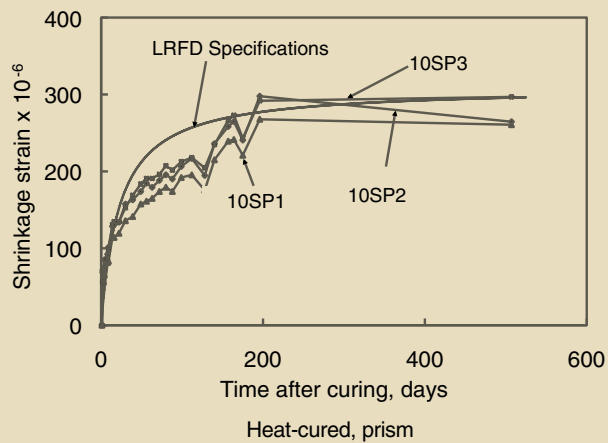
Figure 3. These graphs compare the American Association of State Highway and Transportation Officials' *AASHTO LRFD Bridge Design Specifications* equation with the proposed equation for time-development correction factors for various concrete compressive strengths. Note: f'_{ci} = specified concrete compressive strength at prestress transfer. 1 ksi = 6.895 MPa.

or post-tensioned concrete girders. Accordingly, Eq. (1) is proposed as a replacement to overcome the anomaly associated with the current time-development correction factor k_{id} in the AASHTO LRFD specifications.

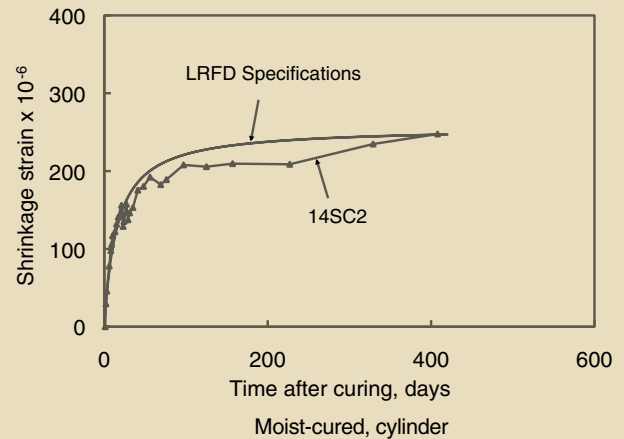
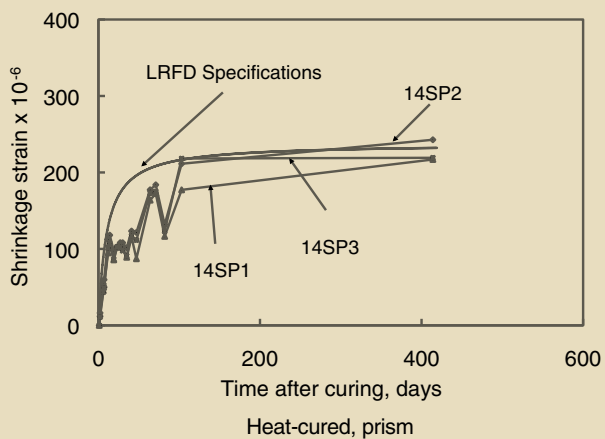
$$k_{id} = \frac{t}{12 \left(\frac{100 - 4f'_{ci}}{f'_{ci} + 20} \right) + t} \quad (1)$$

where

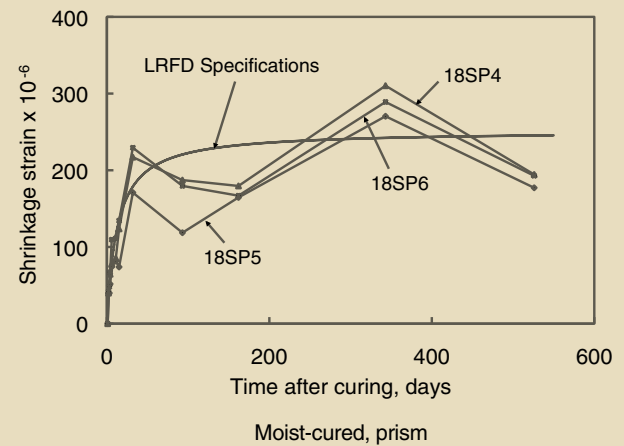
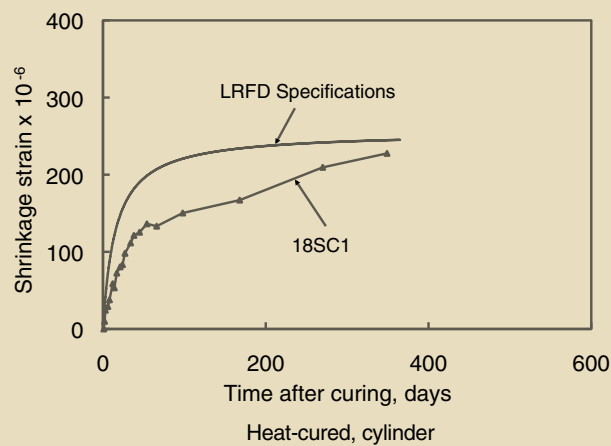
t = age of concrete after loading in days



Set 1 specimens



Set 2 specimens



Set 3 specimens

Figure 4. These graphs compare the adjusted shrinkage strains with the shrinkage strain prediction by the American Association of State Highway and Transportation Officials' AASHTO LRFD Bridge Design Specifications.

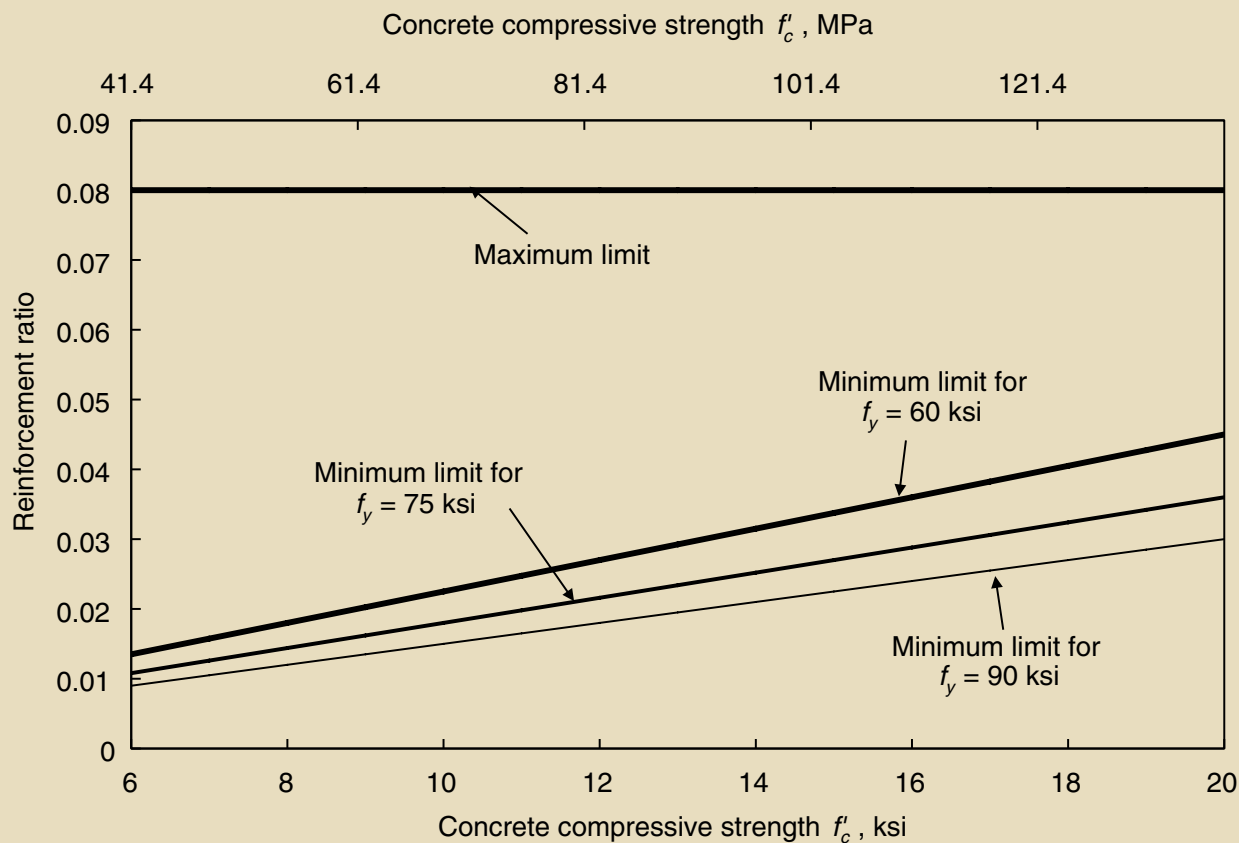


Figure 5. This graph shows the reinforcement limits for compression members with only mild steel according to the American Association of State Highway and Transportation Officials' *AASHTO LRFD Bridge Design Specifications*. Note: f_y = yield strength of mild steel. 1 ksi = 6.895 MPa.

f'_{ci} = specified concrete compressive strength at prestress transfer for prestressed members or 80% of the strength at service for nonprestressed members

Figure 3 compares the proposed time-development correction factor and the AASHTO LRFD specifications' expression for different concrete compressive strengths up to 18 ksi (124 MPa). For concrete compressive strengths greater than 12 ksi (83 MPa), the proposed time-development correction factor eliminates the unreasonable predictions given by the current time-development correction factor, especially for f'_{ci} greater than 14 ksi (97 MPa).

Shrinkage behavior

Shrinkage specimens were monitored at the same time and under the same curing conditions as the creep specimens. The measured shrinkage strains were again adjusted to 70% RH.

Figure 4 compares the adjusted shrinkage strains of the cylindrical and prismatic specimens with the shrinkage strain prediction by the AASHTO LRFD specifications. Only the typical behavior for each of the concrete compressive strengths is presented in this figure due to space limitations. The test results

indicate that there was less shrinkage for heat-cured specimens than for the moist-cured cylinders. The difference in the shrinkage for HSC specimens with concrete compressive strengths ranging from 10 ksi to 18 ksi (69 MPa and 124 MPa) was small. The collected data indicate that the AASHTO LRFD specifications provide reasonably good predictions of shrinkage strains for HSC specimens except that the predicted shrinkage strains are higher than the measured values at an early age.

Minimum reinforcement ratio for compression members

Creep and shrinkage of concrete are important properties that affect the behavior of compression members. The current AASHTO LRFD specifications have two relationships for the limit of the maximum reinforcement and one criterion limiting the minimum reinforcement for compression members (Table 4). The American Concrete Institute's *Building Code Requirements for Structural Concrete (ACI 318-08)* and *Commentary (ACI 318R-08)*⁶ also limits the area of longitudinal reinforcement for noncomposite compression members from $0.01A_g$ to $0.08A_g$ (where A_g is gross area of the section) for all concrete compressive strengths.

The upper limits were initially established based on practical considerations of concrete placement and are applicable for all ranges of concrete compressive strengths. Therefore, it is unnecessary to change the AASHTO LRFD specifications for the maximum reinforcement ratio for compression members.

However, **Fig. 5** shows that the current AASHTO LRFD specifications would require a 4.05% minimum reinforcement ratio for 18 ksi (124 MPa) concrete compressive strength using Grade 60 (60 ksi or 414 MPa) steel for a reinforced concrete column section. Such a high level of required minimum reinforcement ratio is unusual and should be examined for HSC.

For nonprestressed concrete sections, the required minimum longitudinal reinforcement in compression members was established from early column tests by Richart and Staehle.⁷⁻¹⁰ When a column is under sustained service loads, the stress distribution between the steel and the concrete changes over time due to creep and shrinkage of the concrete. With creep and shrinkage increasing progressively, concrete relieves itself from its initial share of the axial load. As a result, longitudinal steel reinforcement gradually carries a larger portion of the sustained load over time. Therefore, it is theoretically possible that in columns with small amounts of longitudinal reinforcement, the reinforcing steel could yield, resulting in creep rupture of the column.

Tests by Richart and Staehle showed that the increase of stress in the steel reinforcement is inversely proportional to the percentage of the longitudinal steel. Results from their tests conducted with concrete compressive strengths from 2 ksi to 8 ksi (14 MPa to 55 MPa) suggested a minimum reinforcement ratio of 1%. The application of this limit was later extended by the AASHTO LRFD specifications for concrete compressive strengths up to 10 ksi (69 MPa) without validation from tests or analysis.

Three types of strain are developed in the longitudinal reinforcement due to the effect of sustained loading: initial elastic strain ε_1 , strain developed due to shrinkage of concrete ε_2 , and strain developed due to creep of concrete ε_3 . To prevent yielding of the longitudinal reinforcement, the summation of the initial elastic strain and the strains due to shrinkage and creep should not reach the yield strain of the longitudinal reinforcement. Therefore

$$\varepsilon_1 + \varepsilon_2 + \varepsilon_3 = \left\{ \frac{P}{A_g \left[E_c (1 - \rho_l) + E_s \rho_l \right]} \right\} + \left\{ \frac{(1 - \rho_l) \varepsilon_{sh} E_c}{\left[\rho_l E_s + (1 - \rho_l) E_c \right]} \right\} + \left\{ \frac{(1 - \rho_l) \varepsilon_{cr} E_c}{\left[\rho_l E_s + (1 - \rho_l) E_c \right]} \right\} \leq \text{Yield strain of longitudinal reinforcement} \quad (2)$$

where

P = applied axial load

E_c = modulus of elasticity of concrete

ρ_l = longitudinal reinforcement ratio

A_g = gross area of concrete

E_s = modulus of elasticity of steel

ε_{sh} = shrinkage strain of concrete

ε_{cr} = creep strain of concrete

For Grade 60 (60 ksi or 414 MPa) steel reinforcement, the yield strain is assumed to be 0.002.

The procedure used to calculate the minimum longitudinal reinforcement ratio for compression members was an iterative procedure that was modeled using Microsoft Excel. The amount of reinforcement was determined for a reinforced concrete column under sustained load, which would lead to a total strain of 0.002 after the specified period of time. The following assumptions and steps were used in the analysis:

1. The modulus of elasticity of steel was taken as 30,000 ksi (200,000 MPa) for Grade 60 (60 ksi or 414 MPa) steel. For the modulus of elasticity of concrete, the relationships proposed by Rizkalla et al.¹¹ as well as the current AASHTO LRFD specifications (Table 4) were used for HSC. Most critical conditions were established using the one proposed by Rizkalla et al. The density of concrete w_c used in the analysis was 0.150 kip/ft³ (2400 kg/m³) because HSC is more compact and denser than normal-strength concrete. Equation (3) was proposed by Rizkalla et al. for modulus of elasticity E_c .

$$310,000 K_1 (w_c)^{2.5} (f'_c)^{0.33} \quad (3)$$

where

K_1 = correction factor for source of aggregate (taken as 1.0)

The analysis was repeated using the current equation specified by the AASHTO LRFD specifications.

2. The shrinkage strain ε_{sh} and creep coefficient ψ relationship specified by the AASHTO LRFD specifications (Table 4) were used to calculate the shrinkage and creep strains of concrete.

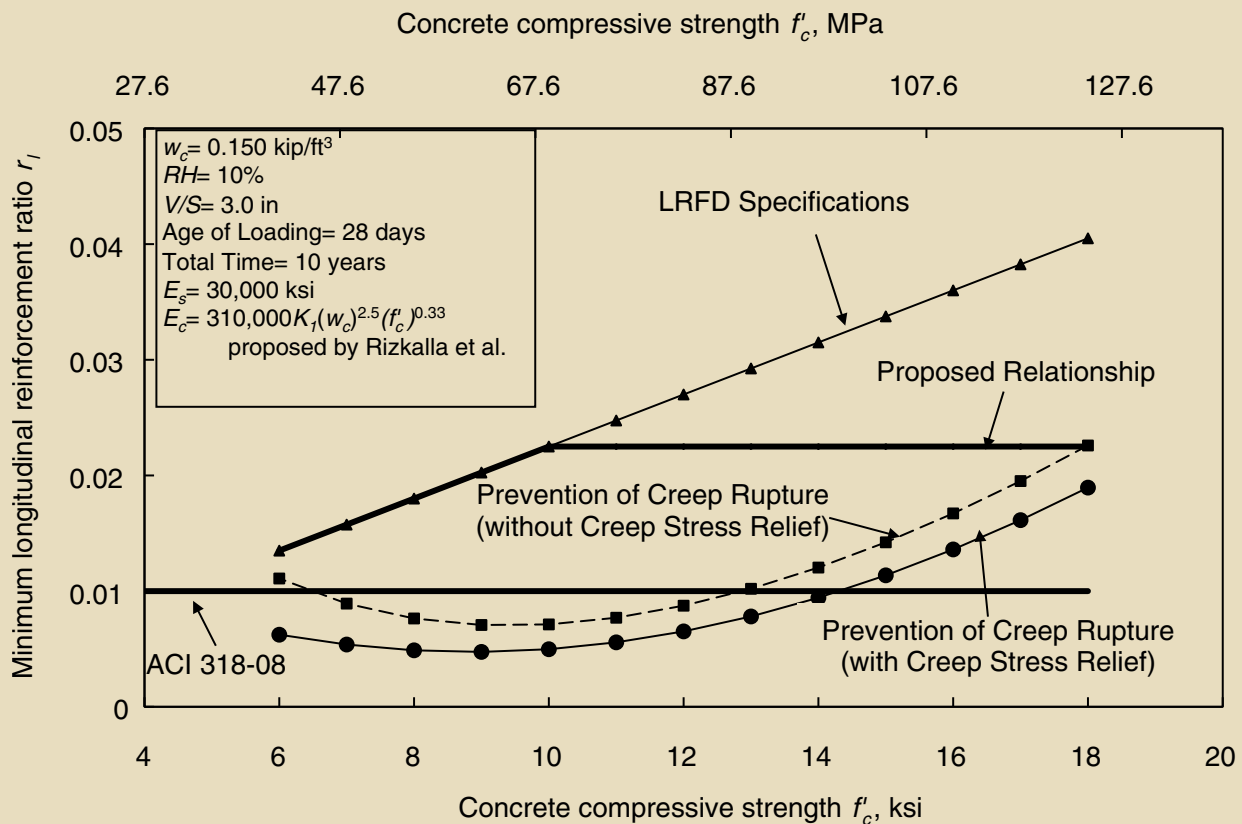


Figure 6. This graph compares the minimum A_s/A_g ratio for $P/f'_c A_g = 0.5$ with and without considering the stress relief due to creep. Note: A_g = gross area of the section of a compression member; A_s = area of mild compression steel; E_c = modulus of elasticity of concrete; E_s = modulus of elasticity of steel; f'_c = target compressive strength of concrete; P = applied axial load; RH = relative humidity; V/S = volume-to-surface ratio; w_c = density of concrete in kip/ft³.

3. The RH used in the calculation of the creep and shrinkage was 10% because a lower RH would produce more-critical results.
 4. The volume-to-surface ratio used in the calculation of creep and shrinkage was 3 in. (75 mm). The volume-to-surface ratio for a circular column with a 12 in. (300 mm) diameter is 3 in. (75 mm). It is the same for a 12 in. \times 12 in. (300 mm \times 300 mm) square column.
 5. The time considered in the calculation of the creep and shrinkage was 10 yr.
 6. The age of loading in the calculation of the creep coefficient was 28 days.
 7. The sustained load level on the reinforced concrete column considered in this investigation was 50% ($P/f'_c A_g = 0.5$). The unfactored permanent load on columns does not exceed $0.5 f'_c A_g$, which is typically the case encountered in design.
 8. The effects associated with stress relief for both creep and shrinkage due to creep of concrete in tension are neglected in the formulation of the equilibrium conditions. By neglecting such effects, the results are more conservative, as shown in **Fig. 6**.
 9. First the initial value for the longitudinal reinforcement ratio ρ_l for a reinforced concrete column was assumed. Then the initial elastic strain and strains due to creep and shrinkage were calculated based on the previous discussions in this section. The sum of all three strain values, the total strain ϵ_{total} , was calculated and compared with the yield strain of steel reinforcement. By changing the initial value of the longitudinal reinforcement ratio, the reinforcement ratio for which the total strain was equal to the yield strain of steel was determined. This reinforcement ratio would be the minimum amount of longitudinal reinforcement ratio for compression members to prevent creep rupture.
 10. Step 9 was performed for all of the concrete compressive strengths in the range of 6 ksi to 18 ksi (41 MPa and 124 MPa).
- The most-critical conditions were evaluated in the calculation of the minimum longitudinal reinforcement ratio for compression members. Based on the analysis using the proposed equation for E_c and the current relationship

Table 5. Comparison of the minimum A_s/A_g ratio for $P/f'_c A_g = 0.5$

f'_c , ksi	Minimum A_s/A_g			
	AASHTO LRFD specifications	ACI 318-08	Proposed	Analytical results
6	0.0135	0.01	0.0135	0.01109
7	0.01575	0.01	0.01575	0.00892
8	0.018	0.01	0.018	0.00764
9	0.02025	0.01	0.02025	0.00707
10	0.0225	0.01	0.0225	0.00712
11	0.02475	0.01	0.0225	0.00770
12	0.027	0.01	0.0225	0.00874
13	0.02925	0.01	0.0225	0.01020
14	0.0315	0.01	0.0225	0.01204
15	0.03375	0.01	0.0225	0.01422
16	0.036	0.01	0.0225	0.01672
17	0.03825	0.01	0.0225	0.01952
18	0.0405	0.01	0.0225	0.02259

Note: A_g = gross area of the section; A_s = area of mild steel; f'_c = compressive strength of concrete; P = applied axial load. 1 ksi = 6.895 MPa.

specified by the AASHTO LRFD specifications, Eq. (4) is proposed as a new relationship for the minimum reinforcement ratio for compression members.

$$\frac{A_s}{A_g} + \frac{A_{ps} f_{pu}}{A_g f_y} \geq 0.135 \frac{f'_c}{f_y} \quad (\text{but not greater than } 0.0225) \quad (4)$$

where

A_s = area of mild-tension steel

A_{ps} = area of prestressing steel

f_{pu} = specified tensile strength of prestressing steel

f_y = yield strength of mild-tension steel

For concrete compressive strengths up to 10 ksi (69 MPa), the proposed relationship for the minimum longitudinal reinforcement ratio requires the same amount as that of the AASHTO LRFD specifications. For concrete compressive strengths greater than 10 ksi (69 MPa), the proposed equation requires the same amount (0.0225) for concrete compressive strengths up to 18 ksi (124 MPa). Furthermore, the proposed minimum reinforcement limitation is similar in format to the maximum reinforcement limitation specified by the AASHTO LRFD specifications.

Table 5 and Fig. 6 show the minimum longitudinal reinforcement ratio for the stress level $P/f'_c A_g$ of 0.5 as required by the current AASHTO LRFD specifications, ACI 318-08,⁶ and the proposed Eq. (4) based on the discussed procedure considering the effects of creep and shrinkage. The figure clearly indicates that for concrete compressive strength greater than 10 ksi (69 MPa), the required minimum longitudinal reinforcement ratio by the proposed equation is much less than that by the current AASHTO LRFD specifications but still provides a substantial margin against what is needed to prevent creep rupture.

Table 6 tabulates the calculated values for minimum reinforcement ratio for compression members to prevent creep rupture for $P/f'_c A_g$ of 0.5. The summation of the initial elastic, shrinkage, and creep strains is equal to the yield strain of 0.002 for Grade 60 (60 ksi or 414 MPa) steel reinforcement. The creep and shrinkage strains of concrete decrease as concrete compressive strength increases. However, the initial elastic strain increases as concrete compressive strength increases because the same stress level was applied on each column with different concrete compressive strengths.

When columns with concrete compressive strengths of 6 ksi and 18 ksi (41 MPa and 124 MPa) are compared under $P/f'_c A_g$ of 0.5, the load applied on the column with a concrete compressive strength of 18 ksi (124 MPa) is three times that applied on the column with a concrete compressive strength of 6 ksi (41 MPa). However, the modulus

Table 6. Calculated values of elastic, shrinkage, and creep strains for $P/f'_c A_g = 0.5$

f'_c , ksi	ρ_l , %	E_c , ksi	Initial elastic strain ϵ_1	Shrinkage strain ϵ_2	Creep strain ϵ_3
6	1.109	4880	0.000582	0.000633	0.000785
7	0.892	5134	0.000653	0.000563	0.000784
8	0.764	5365	0.000720	0.000505	0.000775
9	0.707	5578	0.000782	0.000457	0.000761
10	0.712	5776	0.000841	0.000415	0.000744
11	0.770	5960	0.000895	0.000380	0.000725
12	0.874	6134	0.000946	0.000350	0.000704
13	1.020	6298	0.000994	0.000323	0.000683
14	1.204	6454	0.001039	0.000299	0.000662
15	1.422	6602	0.001081	0.000278	0.000641
16	1.672	6744	0.001122	0.000259	0.000619
17	1.952	6881	0.001159	0.000242	0.000599
18	2.259	7012	0.001195	0.000227	0.000578

Note: A_g = gross area of the section; E_c = elastic modulus of concrete; f'_c = compressive strength of concrete; P = applied axial load; ρ_l = longitudinal reinforcement ratio. 1 ksi = 6.895 MPa.

of elasticity of the column with a concrete compressive strength of 18 ksi (124 MPa) is only 1.44 times that of the column with a concrete compressive strength of 6 ksi (41 MPa). Therefore, the minimum reinforcement ratio for compression members cannot be reduced for HSC compared with normal-strength concrete, though the creep and shrinkage are less for HSC.

Conclusion

A total of 42 cylindrical specimens and 18 prismatic specimens were tested for up to two years to evaluate the creep and shrinkage behavior of HSC. The variables considered in this investigation were concrete compressive strengths from 10 ksi to 18 ksi (69 MPa to 124 MPa), specimen shape (cylinder or prism), curing type (moist or heat curing), age of concrete at loading (1 day, 7 days, 14 days, or 28 days), and loading stress level ($0.2 f'_c$ or $0.4 f'_c$). The creep coefficient and shrinkage strain were obtained for the range of concrete compressive strengths, evaluated, and compared with the predictions by the AASHTO LRFD specifications. Several conclusions were made:

- The creep behavior of HSC is similar to that of normal-strength concrete, where creep rate decreases as time increases.
- For the same concrete compressive strength, the creep of the 1-day heat-cured cylinders is less than that of the 7-day moist-cured cylinders.
- AASHTO LRFD specifications overestimate creep coefficients for heat-cured HSC specimens, but the AASHTO LRFD specifications produced closer predictions for moist-cured HSC specimens.
- The relationships specified by the AASHTO LRFD specifications are reasonable for predicting creep of HSC, except for the time-development correction factor k_{td} , which produces negative values in the first few days after loading if the concrete compressive strength is greater than 15 ksi (103 MPa). Accordingly, a new time-development correction factor (Eq. [1]) was developed to overcome the anomaly associated with the current time-development correction factor.
- Heat-cured specimens have less shrinkage compared with moist-cured specimens.
- The difference in the shrinkage for HSC specimens with concrete compressive strengths ranging from 10 ksi to 18 ksi (69 MPa and 124 MPa) is small.
- AASHTO LRFD specifications predict the shrinkage of HSC specimens well.
- For HSC, the current AASHTO LRFD specifications would require unusually high amounts of minimum longitudinal reinforcement for nonprestressed, non-composite concrete compression members. Based on the analysis presented in this paper, a new relationship

(Eq. [4]) was proposed for the minimum reinforcement ratio for compression members.

Acknowledgments

The authors acknowledge the support of the NCHRP project 12-64 and the senior program officer, David Beal. They are also grateful for the contributions of Henry Russell of Henry Russell Inc. and Robert Mast of Berger/ABAM Engineers Inc., who served as consultants for the project. The cooperation of Ready Mixed Concrete Co. of Raleigh, N.C., and the support of the personnel of the Constructed Facilities Laboratory are also greatly appreciated. The assistance provided by Andrew Logan, Sung Joong Kim, Zhenhua Wu, and Wonchang Choi during all aspects of the research program was crucial to the success of the project.

References

1. American Association of State Highway and Transportation Officials (AASHTO). 2004. *AASHTO LRFD Bridge Design Specifications*. 3rd ed. Washington, DC: AASHTO.
2. Tadros, M. K., N. Al-Omaishi, S. J. Seguirant, and J. G. Gallt. 2003. *Prestress Losses in Pretensioned High-Strength Concrete Bridge Girders*. National Cooperative Highway Research Program (NCHRP) report 496. Washington, DC: Transportation Research Board.
3. Logan, A. T. 2005. Short-Term Material Properties of High-Strength Concrete. MS thesis. Department of Civil, Construction and Environmental Engineering, North Carolina State University, Raleigh, NC.
4. ASTM C 157/C 157M. 2008. *Standard Test Method for Length Change of Hardened Hydraulic-Cement Mortar and Concrete*. West Conshohocken, PA: ASTM International.
5. Mertol, H. C. 2006. Characteristics of High Strength Concrete for Combined Flexure and Axial Compression Members. PhD thesis. Department of Civil, Construction and Environmental Engineering, North Carolina State University, Raleigh, NC.
6. American Concrete Institute (ACI) 318. 2008. *Building Code Requirements for Structural Concrete (ACI 318-08) and Commentary (ACI 318R-08)*. Farmington Hills, MI: ACI.
7. Richart, F. E., and G. C. Staehle. 1931. Progress Report on Column Tests at the University of Illinois. *Journal of the American Concrete Institute*, V. 27: pp. 731–760.
8. Richart, F. E., and G. C. Staehle. 1931. Second Progress Report on Column Tests at the University of

Illinois. *Journal of the American Concrete Institute*, V. 27: pp. 761–790.

9. Richart, F. E., and G. C. Staehle. 1931. Third Progress Report on Column Tests at the University of Illinois. *Journal of the American Concrete Institute*, V. 28: pp. 167–175.
10. Richart, F. E., and G. C. Staehle. 1932. Fourth Progress Report on Column Tests at the University of Illinois. *Journal of the American Concrete Institute*, V. 28: pp. 279–315.
11. Rizkalla, S., A. Mirmiran, P. Zia, H. Russell, and R. Mast. 2007. *Application of the LRFD Bridge Design Specifications to High-Strength Structural Concrete: Flexure and Compression Provisions*. NCHRP report 595. Washington, DC: Transportation Research Board.

Notation

- A_g = gross area of the section of a compression member
- A_{ps} = area of prestressing steel
- A_s = area of mild steel
- E_c = modulus of elasticity of concrete
- E_s = modulus of elasticity of steel
- f'_c = target compressive strength of concrete
- f'_{ci} = specified concrete compressive strength at prestress transfer for prestressed members or 80% of the strength at service for nonprestressed members
- f_{pe} = effective stress in prestressing steel after losses
- f_{pu} = specified tensile strength of prestressing steel
- f_y = yield strength of mild steel
- k_f = concrete strength factor
- k_{hc} = humidity factor for creep coefficient
- k_{hs} = humidity factor for shrinkage strain
- k_{la} = loading-age factor
- k_s = size factor
- k_{td} = time-development correction factor

K_1 = correction factor for source of aggregate (taken as 1.0 if source is unknown)

P = applied axial load

RH = relative humidity

t = age of concrete after loading in days

t_i = age of concrete when load is initially applied in days

V/S = volume-to-surface ratio

w_c = density of concrete

w/c = water-to-cement ratio

ε_1 = initial elastic strain in concrete

ε_2 = strain developed in concrete due to shrinkage

ε_3 = strain developed in concrete due to creep

ε_{cr} = creep strain of concrete

ε_{sh} = shrinkage strain of concrete

ε_{total} = total strain = $\varepsilon_1 + \varepsilon_2 + \varepsilon_3$

ρ_l = longitudinal reinforcement ratio in column

ψ = creep coefficient

About the authors



Halit Cenan Mertol, PhD, is an assistant professor for the Department of Civil Engineering at Atilim University in Ankara, Turkey.



Sami Rizkalla, PhD, P.Eng., FPCI, is a Distinguished Professor of Civil, Construction, and Environmental Engineering and director of the Constructed Facilities Laboratory at North Carolina State University in Raleigh, N.C.



Paul Zia, PhD, P.E., FPCI, is a Distinguished University Professor Emeritus at North Carolina State University in Raleigh, N.C.



Amir Mirmiran, PhD, P.E., is a professor of Civil Engineering and interim dean of Engineering at Florida International University in Coral Gables, Fla.

Synopsis

This paper summarizes the findings of an extensive research program that examined the shrinkage and creep behavior of high-strength concrete (HSC) up to a strength of 18 ksi (124 MPa). Creep and shrinkage strains of 60 specimens were monitored for up to two years. The variables considered in this investigation were the concrete compressive strength, specimen

size, curing type, age of concrete at loading, and loading stress level.

Research findings indicate that the current American Association of State Highway and Transportation Officials' *AASHTO LRFD Bridge Design Specifications* could be used to estimate the creep coefficient and shrinkage strain of HSC up to 15 ksi (103 MPa). However, the current AASHTO LRFD specifications do not provide appropriate predictions for concrete compressive strength greater than 15 ksi (103 MPa). A revised time-development correction factor is proposed to obtain better predictions for HSC up to 18 ksi (124 MPa).

For HSC compression members, the current AASHTO LRFD specifications require an excessive amount of minimum longitudinal reinforcement to account for the long-term effects due to shrinkage and creep. Based on an analysis, a new relationship is proposed for the required minimum reinforcement ratio.

Keywords

Column, creep, high-strength concrete, longitudinal reinforcement ratio, shrinkage.

Review policy

This paper was reviewed in accordance with the Precast/Prestressed Concrete Institute's peer-review process.

Reader comments

Please address any reader comments to *PCI Journal* editor-in-chief Emily Lorenz at elorenz@pci.org or Precast/Prestressed Concrete Institute, c/o *PCI Journal*, 200 W. Adams St., Suite 2100, Chicago, IL 60606. 